

Mechanistic Studies on the Cyclization of Organosilicon and Organotin Compounds Containing the O,C,O-Coordinating Pincer-Type Ligand {4-*t*-Bu-2,6-[P(O)(OR)₂]₂C₆H₂}⁻ (R = *i*-Pr, Et): Phosphorus (POC)- versus Carbon (POC)-Attack[†]

Katja Peveling, Markus Henn, Christian Löw, Michael Mehring, Markus Schürmann, Burkhard Costisella, and Klaus Jurkschat*

Lehrstuhl für Anorganische Chemie II der Universität Dortmund,
D-44221 Dortmund, Germany

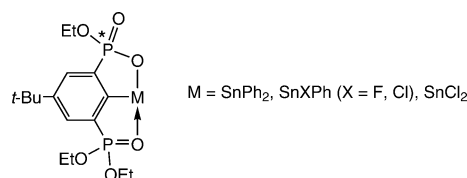
Received July 1, 2003

The intramolecularly coordinated triorganotin hexafluorophosphate {4-*t*-Bu-2,6-[P(O)(*Oi*-Pr)₂]₂C₆H₂}SnPh₂⁺PF₆⁻ (**3a**) was prepared by reaction of the [4+2]-coordinated tetraorganotin compound {4-*t*-Bu-2,6-[P(O)(*Oi*-Pr)₂]₂C₆H₂}SnPh₃ (**2a**) with Ph₃C⁺PF₆⁻ and shown to react under intramolecular cyclization with bromide and fluoride ion, respectively, as well as with water to give the intramolecularly coordinated benzoxaphosphastannole [1(P),3(Sn)-SnPh₂-OP(O)(*Oi*-Pr)-6-*t*-Bu-4-P(O)(*Oi*-Pr)₂]₂C₆H₂ (**4a**). Analogously, the in situ-generated intramolecularly coordinated triorganosiliconium hexafluorophosphate {4-*t*-Bu-2,6-[P(O)(OEt)₂]₂-C₆H₂}SiPh₂⁺PF₆⁻ (**6**) reacts with water to give the corresponding intramolecularly coordinated benzoxaphosphasilole [1(P),3(Si)-P(O)(OEt)OSiPh₂-6-*t*-Bu-4-P(O)(OEt)₂]₂C₆H₂ (**7**). Isotope-labeling experiments with H₂¹⁸O in combination with electrospray mass spectrometric studies reveal that in the case of the organotin compound **3a** the cyclization exclusively proceeds via nucleophilic attack of water at the POC-carbon. In contrast, two pathways account for the formation of the benzoxaphosphasilole **7**, that is, attack of water at the POC-carbon as well as at phosphorus. The latter pathway either is in contrast to the axial entry–axial departure principle of nucleophilic substitution at phosphorus or indicates Berry pseudorotation involving a five-membered chelate ring. The molecular structure of **3a** was determined by single-crystal X-ray diffraction analysis.

Introduction

Recently we reported the application of the O,C,O-coordinating pincer-type ligand {4-*t*-Bu-2,6-[P(O)(OR)₂]₂-C₆H₂}⁻ (**A**, R = *i*-Pr; **B**, R = Et) for the synthesis of a series of hypercoordinated organosilicon,^{1–3} organotin,^{4–6} and organolead⁷ compounds. One characteristic feature of these compounds is that reactions at both the metal and the phosphinyl moieties^{3,5,6} are possible. Thus, the reaction of the [4+2]-coordinated tetraorga-

Chart 1



notin derivative {4-*t*-Bu-2,6-[P(O)(OEt)₂]₂C₆H₂}SnPh₃ with iodine gave the hypercoordinated benzoxaphosphastannole [1(P),3(Sn)-SnPh₂OP(O)(OEt)-6-*t*-Bu-4-P(O)(OEt)₂]₂C₆H₂ (Chart 1) and not, as originally expected, the hypercoordinated triorganotin iodide {4-*t*-Bu-2,6-[P(O)(OEt)₂]₂C₆H₂}SnIPh₂.⁵ Furthermore, heating toluene solutions of the hypercoordinated diorganotin dihalides and monoorganotin trichloride {4-*t*-Bu-2,6-[P(O)(OEt)₂]₂C₆H₂}SnX₂Ph (X = F, Cl) and {4-*t*-Bu-2,6-[P(O)(OEt)₂]₂C₆H₂}SnCl₃, respectively, provided the halogen-substituted hypercoordinated benzoxaphosphastannoles [1(P),3(Sn)-Sn(X)(Y)OP(O)(OEt)-6-*t*-Bu-4-P(O)(OEt)₂]₂C₆H₂ (X = F, Cl, Y = Ph; X = Y = Cl, Ph) (Chart 1).⁶

These results were interpreted in terms of hypercoordinated organotin cations (Chart 2) to be intermediates in these intramolecular cyclization reactions. Later on we learned that the in situ-generated hypercoordi-

[†] This work contains parts of the Ph.D. theses of K. Peveling, Dortmund, 2003, and of M. Henn, Dortmund, 2004.

* Corresponding author. Tel: 49-231-7553800. Fax: 49-231-7555048. E-mail: kjur@platon.chemie.uni-dortmund.de.

(1) Mehring, M.; Jurkschat, K.; Schürmann, M. *Main Group Met. Chem.* **1998**, *21*, 635.

(2) Peveling, K.; Schürmann, M.; Jurkschat, K. *Main Group Met. Chem.* **2001**, *24*, 251.

(3) Peveling, K.; Schürmann, M.; Ludwig, R.; Jurkschat, K. *Organometallics* **2001**, *20*, 4654. In this paper the nomenclature used was not correct (for instance benzoxasilaphosphole instead of benzoxaphosphasilole). We thank an anonymous reviewer for making us aware of this.

(4) Mehring, M.; Schürmann, M.; Jurkschat, K. *Organometallics* **1998**, *17*, 1227.

(5) Mehring, M.; Löw, C.; Schürmann, M.; Jurkschat, K. *Eur. J. Inorg. Chem.* **1999**, 887.

(6) Mehring, M.; Vrasidas, I.; Horn, D.; Schürmann, M.; Jurkschat, K. *Organometallics* **2001**, *20*, 4647.

(7) Peveling, K.; Schürmann, M.; Jurkschat, K. *Z. Anorg. Allg. Chem.* **2002**, *628*, 2435.

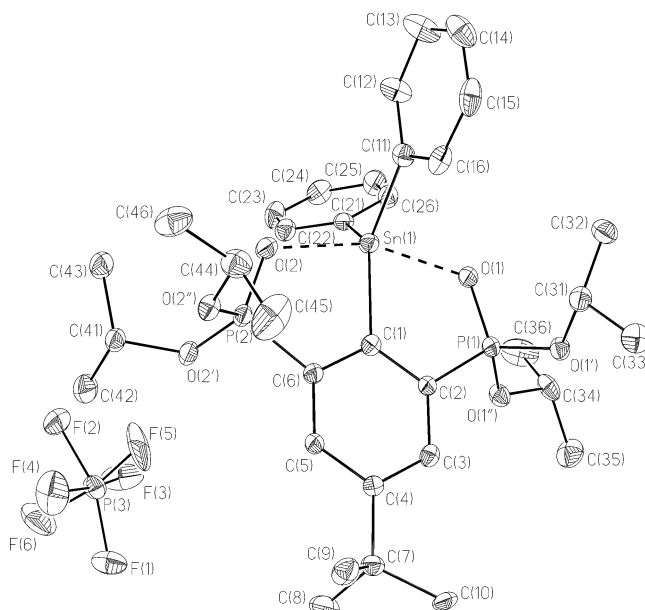
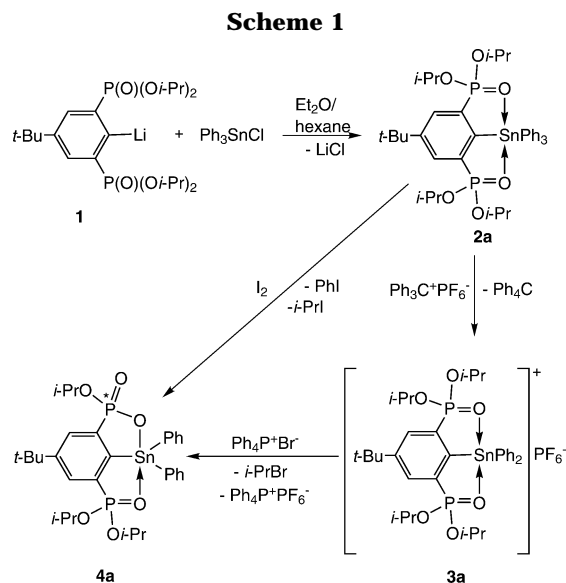
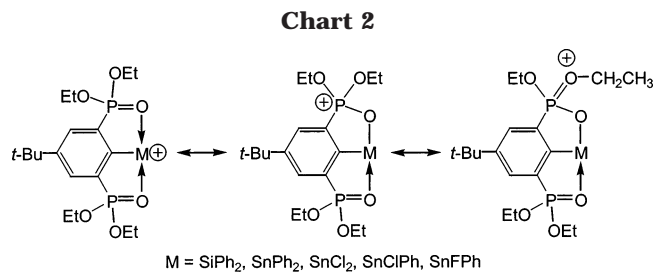


Figure 1. General view (SHELXTL) of a molecule of **3a** showing 30% probability displacement ellipsoids and the atom numbering.

Compound **2a** reacts with triphenylcarbonium hexafluorophosphate, $\text{Ph}_3\text{C}^+\text{PF}_6^-$, to give the hypercoordinated triorganotin hexafluorophosphate $\{4\text{-}t\text{-Bu-2,6-}[\text{P}(\text{O})(\text{O}i\text{-Pr})_2]_2\text{C}_6\text{H}_2\}\text{SnPh}_2^+\text{PF}_6^-$ (**3a**) (Scheme 1).

The molecular structure of compound **3a** is shown in Figure 1, relevant crystallographic parameters are given in the Experimental Section, and selected geometrical data are listed in Table 1.

The unit cell of compound **3a** contains two cation–anion pairs. The separation between the triorganotin cation, $\{4\text{-}t\text{-Bu-2,6-}[\text{P}(\text{O})(\text{O}i\text{-Pr})_2]_2\text{C}_6\text{H}_2\}\text{SnPh}_2^+$, and the hexafluorophosphate anion, PF_6^- , amounts to 8.9048(14) Å and indicates no bonding interaction.

The tin atom shows a trigonal bipyramidal configuration (geometrical goodness^{11–13} $\Delta\Sigma(\theta) = 84.6^\circ$) with C(1), C(11), and C(21) in equatorial and O(1) and O(2) in axial positions. The O(1)–Sn(1)–O(2) angle amounts to 159.01(9)°, which is comparable to the corresponding angles in hexacoordinated $[\{4\text{-}t\text{-Bu-2,6-}[\text{P}(\text{O})(\text{O}i\text{-Pr})_2]_2\text{C}_6\text{H}_2\}\text{Sn}(\text{Cl})\text{S}]_2$ (159.0(1)°),¹⁴ $\{4\text{-}t\text{-Bu-2,6-}[\text{P}(\text{O})(\text{O}i\text{-Pr})_2]_2\text{C}_6\text{H}_2\}\text{SnX}_2\text{Ph}$ (X = Cl, 161.1(2)°; X = F, 159.8(1)°),^{4,6} and $\{4\text{-}t\text{-Bu-2,6-}[\text{P}(\text{O})(\text{O}i\text{-Pr})_2]_2\text{C}_6\text{H}_2\}\text{SnCl}_3$ (161.1(1)°).⁵

The intramolecular Sn(1)–O(1) and Sn(1)–O(2) distances amount to 2.249(2) and 2.241(3) Å, respectively, reflecting Pauling-type bond orders^{15–17} of 0.68 and 0.70. These distances are 39% shorter than the sum of the

nated triorganosiliconium cation $\{4\text{-}t\text{-Bu-2,6-}[\text{P}(\text{O})(\text{O}i\text{-Pr})_2]_2\text{C}_6\text{H}_2\}\text{SiPh}_2^+$ (Chart 2) reacts with water in a similar manner to give the hypercoordinated benzoxaphosphasilole $[\text{1}(\text{P}),\text{3}(\text{Si})\text{-P}(\text{O})(\text{O}i\text{-Pr})\text{OSiPh}_2\text{-6-}t\text{-Bu-4-P}(\text{O})(\text{O}i\text{-Pr})_2]_2\text{C}_6\text{H}_2$.³ The formation of the latter compound involves nucleophilic attack of water at the triorganosiliconium ion, but the position of this attack is not clear, and one anonymous reviewer of our previous paper³ suggested we look at this problem in more detail.

In this paper we report the synthesis and structure of the hypercoordinated triorganotin cation $\{4\text{-}t\text{-Bu-2,6-}[\text{P}(\text{O})(\text{O}i\text{-Pr})_2]_2\text{C}_6\text{H}_2\}\text{SnPh}_2^+$, as its hexafluorophosphate **3a**, and show that it reacts with bromide and fluoride ion as well as with water to give the hypercoordinated benzoxaphosphastannole $[\text{1}(\text{P}),\text{3}(\text{Sn})\text{-SnPh}_2\text{OP}(\text{O})(\text{O}i\text{-Pr})\text{-6-}t\text{-Bu-4-P}(\text{O})(\text{O}i\text{-Pr})_2]_2\text{C}_6\text{H}_2$ (**4a**).

Furthermore we show by means of ¹⁸O-labeling experiments and supported by electrospray mass spectrometry (ESMS) that the position at which the water attacks the cation $\{4\text{-}t\text{-Bu-2,6-}[\text{P}(\text{O})(\text{OR})_2]_2\text{C}_6\text{H}_2\}\text{MPh}_2^+\text{PF}_6^-$ (M = Si, Sn; R = *i*-Pr, Et) is controlled by the identity of the element M.

Noteworthy, reactions of halide ions with intramolecularly coordinated siliconium ions giving rise to N–C^{8,9} and O–C bond cleavage,¹⁰ respectively, have also been reported recently.

Results and Discussion

Reaction of the in situ-generated organolithium compound **1** with Ph_3SnCl provided $\{4\text{-}t\text{-Bu-2,6-}[\text{P}(\text{O})(\text{O}i\text{-Pr})_2]_2\text{C}_6\text{H}_2\}\text{SnPh}_3$ (**2a**) in good yield (Scheme 1).

(8) Mickoleit, M. *Synthese, Struktur und Reaktivität donorstabilisierter Silene*. Dissertation Universität Rostock, Rostock, Germany, 2002.

(9) Kost, D.; Gostevskii, B.; Kocher, N.; Stalke, D.; Kalikhman, I. *Angew. Chem.* **2003**, *115*, 1053; *Angew. Chem., Int. Ed.* **2003**, *42*, 1023.

(10) Berlekamp, U. H.; Mix, A.; Jutzki, P.; Stammner, H. G.; Neumann, B. Oxygen, Phosphorus or Sulfur Donor Ligands in Higher-Coordinated Organosilyl Chlorides and Triflates. In *Organosilicon Chemistry IV*; Auner, N., Weiss, J., Eds.; Wiley-VCH: New York, 2000; p 489.

(11) Kolb, U.; Dräger, M.; Jousseume, B. *Organometallics* **1991**, *10*, 2737.

(12) Kolb, U.; Beuter, M.; Dräger, M. *Inorg. Chem.* **1994**, *33*, 4522.

(13) Kolb, U.; Beuter, M.; Gerner, M.; Dräger, M. *Organometallics* **1994**, *13*, 4413.

(14) Mehring, M.; Löw, C.; Schürmann, M.; Uhlig, F.; Jurkschat, K.; Mahieu, B. *Organometallics* **2000**, *19*, 4613.

(15) Pauling, L. *The Nature of the Chemical Bond*, 3rd ed.; Cornell University Press: Ithaca, New York, 1960.

(16) Dunitz, J. D. *X-Ray Analysis and the Structure of Organic Molecules*; Cornell University Press: Ithaca, New York, 1979.

Table 1. Selected Bond Lengths (Å), Bond Angles (deg), and Torsion Angles (deg) for **3a**

Sn(1)–C(1)	2.132(4)
Sn(1)–C(11)	2.116(4)
Sn(1)–C(21)	2.114(3)
Sn(1)–O(1)	2.249(2)
Sn(1)–O(2)	2.241(3)
P(1)–O(1)	1.501(3)
P(2)–O(2)	1.497(3)
P(1)–O(1')	1.553(3)
P(1)–O(1'')	1.555(3)
P(2)–O(2')	1.539(3)
P(2)–O(2'')	1.552(3)
C(11)–Sn(1)–C(1)	119.9(1)
C(21)–Sn(1)–C(1)	125.8(1)
C(21)–Sn(1)–C(11)	114.1(1)
C(1)–Sn(1)–O(1)	79.3(1)
O(2)–Sn(1)–C(1)	79.7(1)
C(11)–Sn(1)–O(1)	93.8(1)
O(2)–Sn(1)–C(11)	97.4(1)
C(21)–Sn(1)–O(1)	93.4(1)
O(2)–Sn(1)–C(21)	98.1(1)
O(2)–Sn(1)–O(1)	159.01(9)
O(1)–P(1)–C(2)	106.7(2)
O(2)–P(2)–C(6)	106.4(2)
P(1)–O(1)–Sn(1)	118.1(1)
P(2)–O(2)–Sn(1)	118.8(1)
P(2)–C(6)–C(1)	115.0(3)
P(1)–C(2)–C(1)	114.6(3)
C(6)–C(1)–Sn(1)	120.0(3)
C(2)–C(1)–Sn(1)	121.2(3)
C(5)–C(6)–C(1)–Sn(1)	179.0(2)
C(3)–C(2)–C(1)–Sn(1)	–178.7(2)
C(5)–C(6)–P(2)–O(2)	–176.4(3)
C(3)–C(2)–P(1)–O(1)	179.7(3)

van der Waals radii of tin and oxygen (3.700 Å)¹⁷ and notably shorter than the corresponding distances in the [4+2]-coordinated tetraorganotin compound {4-*t*-Bu-2,6-[P(O)(OEt)₂]₂C₆H₂}SnPh₃ (2.865(3), 3.063(4) Å),⁴ but close to the Sn–O distances in hexacoordinated {4-*t*-Bu-2,6-[P(O)(OEt)₂]₂C₆H₂}SnCl₂R (R = Ph, Cl) falling in the range between 2.203(5) and 2.278(6) Å.^{4,5} The strong intramolecular Sn–O interactions in compound **3a** are also reflected by the C(1)–C(2)–P(1) and C(1)–C(6)–P(2) angles (defined as α, α' angles¹⁸) of 114.6(3)° and 115.0(3)°, respectively, being 4.6° and 4.7° smaller than the corresponding angles in the tetraorganotin compound {4-*t*-Bu-2,6-[P(O)(OEt)₂]₂C₆H₂}SnPh₃.⁴ The P(O)(O*i*-Pr)₂ groups are displaced in one direction and the tin atom is displaced in the opposite direction of the plane defined by the aromatic ring (torsion angles P(1)–C(2)–C(3)–C(4) = –176.4(3)° and Sn(1)–C(1)–C(2)–C(3) = 178.7(2)°). The IR spectrum of the hypercoordinated triorganotin hexafluorophosphate **3a** shows a $\tilde{\nu}(\text{P}=\text{O})$ absorption at 1177 cm^{–1}, which corresponds to P(1)–O(1) and P(2)–O(2) distances of 1.501(3) and 1.497(3) Å and which is almost identical to the $\tilde{\nu}(\text{P}=\text{O})$ of 1176 and 1170 cm^{–1}, respectively, measured for {4-*t*-Bu-2,6-[P(O)(OEt)₂]₂C₆H₂}SnCl₂R (R = Ph, Cl, P=O distances in the range between 1.493(5) and 1.506(5) Å).^{4,5} Comparable P=O distances of 1.500(3) and 1.491(2) Å were reported for {Ph₃Sn[P(O)(NMe₂)₃]₂}⁺{N[S(O)₂Me]₂}[–].¹⁹

(17) Huheey, J.; Keiter, E. A.; Keiter, R. L. *Anorganische Chemie: Prinzipien von Struktur und Reaktivität*, 2 ed.; de Gruyter: New York, 1995.

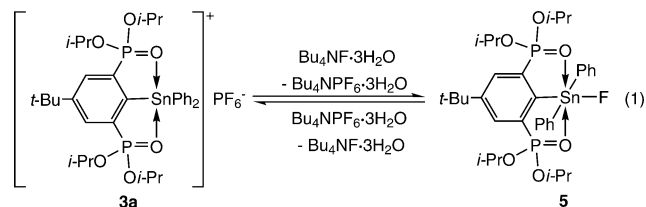
(18) Henn, M.; Jurkschat, K.; Ludwig, R.; Mehring, M.; Peveling, K.; Schürmann, M. *Z. Anorg. Allg. Chem.* **2002**, *628*, 2940.

(19) Lange, I.; Henschel, D.; Wirth, A.; Krahl, J.; Blaschette, A.; Jones, P. G. *J. Organomet. Chem.* **1995**, *503*, 155.

The ¹¹⁹Sn NMR spectrum of the triorganotin hexafluorophosphate **3a** exhibits a triplet resonance at δ ¹¹⁹Sn = –207.8 ($J(^{119}\text{Sn}-^{31}\text{P}) = 5$ Hz), which is close to its ¹¹⁹Sn MAS NMR shift of –200.4 ppm, indicating similar structures in solution and in the solid state.

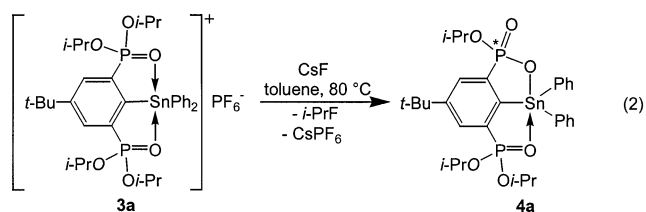
Treatment in toluene of the hypercoordinated triorganotin hexafluorophosphate **3a** with tetraphenylphosphonium bromide, Ph₄PBr (Scheme 1), provided a crude reaction mixture, the ³¹P NMR spectrum of which exhibited two equally intense doublet resonances at δ 16.5 ($J(^{31}\text{P}-^{31}\text{P}) = 3$ Hz) and δ 26.6 ($J(^{31}\text{P}-^{31}\text{P}) = 3$ Hz). These data unambiguously indicate formation of the hypercoordinated benzoxaphosphastannole [1(P),3(Sn)-SnPh₂OP(O)(O*i*-Pr)-6-*t*-Bu-4-P(O)(O*i*-Pr)₂]C₆H₂ (**4a**). Compound **4a** was not isolated from this reaction mixture but was obtained in good yield, like its ethoxy-substituted analogue **4b**,⁵ by reaction of the [4+2]-coordinated tetraorganotin compound **2a** with iodine (Scheme 1).

The ¹¹⁹Sn NMR spectrum (CD₂Cl₂) at –30 °C of the hypercoordinated triorganotin hexafluorophosphate **3a** to which had been added 1 molar equiv of tetrabutylammonium fluoride water adduct, Bu₄NF·3H₂O, revealed a broad singlet resonance at δ –211.3 ($\nu_{1/2} = 24$ Hz), integral 42, **3a**) and a doublet of triplet resonance at δ –267.7 ($J(^{119}\text{Sn}-^{31}\text{P}) = 39$ Hz, $J(^{119}\text{Sn}-^{19}\text{F}) = 2354$ Hz, integral 58). The latter signal is assigned to the hexacoordinated triorganotin fluoride {4-*t*-Bu-2,6-[P(O)(O*i*-Pr)₂]₂C₆H₂}SnFPh₂ (**5**) (eq 1).



Addition of a second molar equivalent of Bu₄NF·3H₂O shifts the equilibrium according to eq 1 completely to the right. To the best of our knowledge, compound **5** is the first example of a hexacoordinated triorganotin compound in solution. The existence of such compounds in the solid state was established by single-crystal X-ray analysis for N[(CH₂)₃]₃SnF·H₂O²⁰ and [8-Me₂N-1-C₁₀H₆]₂-SnIme.²¹

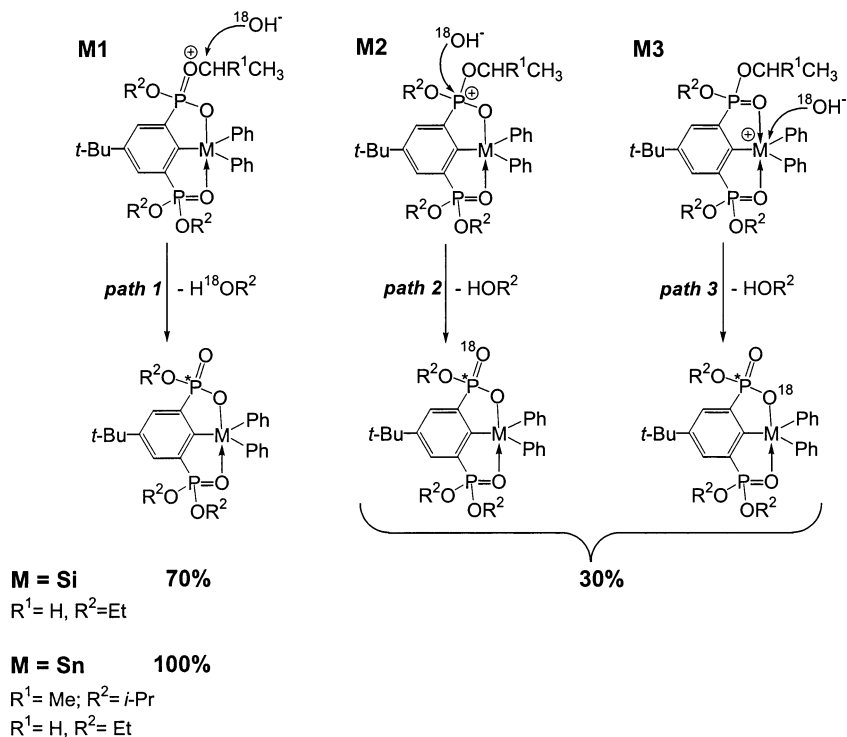
The ³¹P NMR spectrum (toluene) of a mixture of the hypercoordinated triorganotin hexafluorophosphate **3a** and water-free CsF revealed, after the reaction mixture had been heated for 12 h at 80–90 °C, almost complete formation of the benzoxaphosphastannole **4a** and *i*-PrF (eq 2).



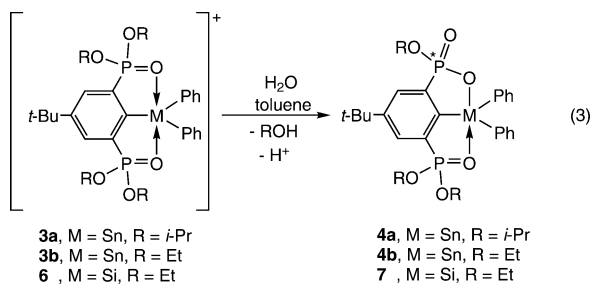
(20) Kolb, U.; Dräger, M.; Dargatz, M.; Jurkschat, K. *Organometallics* **1995**, *14*, 2827.

(21) Jastrzebski, J. T. B. H.; van der Schaaf, P. A.; Boersma, J.; van Koten, G.; de Ridder, D. J. A.; Heijdenrijk, D. *Organometallics* **1992**, *11*, 1521.

Scheme 2



As it was reported in an earlier paper, the in situ-generated triorganosiliconium cation **6** reacts with water to give the hypercoordinated benzoxaphosphasilole [1(P),3(Si)-P(O)(OEt)OSiPh₂-6-*t*-Bu-4-P(O)(OEt)₂]C₆H₂ (**7**) (eq 3).³ The same type of reaction takes place upon addition of water to a solution of the hypercoordinated triorganotin cations **3a** and **3b** and heating these at 80 °C for 48 h, providing the hypercoordinated benzoxaphosphastannoles [1(P),3(Sn)-SnPh₂OP(O)(OR)-6-*t*-Bu-4-P(O)(OR)₂]C₆H₂ (**4a**, R = *i*-Pr; **4b**, R = Et) (eq 3).



The formation of the heterocycles **4a**, **4b**, and **7** can be rationalized by nucleophilic attack of a water molecule either at the POC-carbon in the canonical structure **M1**, at the phosphorus atom (canonical structure **M2**), or at the metal atom (canonical structure **M3**) followed by release of ethanol or isopropanol, respectively (Scheme 2). By use of ¹⁸O-labeled water, H₂¹⁸O (95% ¹⁸O), at least path 1 involving **M1** should be distinguishable from paths 2 and 3 involving **M2** and **M3**, respectively. While the attack of H₂¹⁸O at the POC-carbon (path 1) results in formation of R¹⁸OH (R = Et, *i*-Pr), the ¹⁸O atom is incorporated into the benzoxaphosphastannoles or benzoxaphosphasiloles, respectively, if path 2 or path 3 is operative (Scheme 2).

The electrospray mass spectrum (ESMS) of the benzoxaphosphastannole derivatives [1(P),3(Sn)-SnPh₂OP-

(O)(OR)-6-*t*-Bu-4-P(O)(OR)₂]C₆H₂ (**4a**, R = *i*-Pr; **4b**, R = Et), which were prepared by reaction of the triorganotin cations **3a** and **3b**, respectively, with H₂¹⁸O did not show the incorporation of additional ¹⁸O above the natural abundance and revealed the reaction to proceed via path 1.

In contrast, the ESMS of the corresponding benzoxaphosphasilole **7**, which was prepared by reaction of the in situ-generated triorganosiliconium cation **6** with H₂¹⁸O, revealed formation of 30% (above natural abundance) ¹⁸O-containing benzoxaphosphasilole **7** (Figure 2). Apparently, both path 1 and path 2 or path 3 are operative, one of the two latter accounting for the increased ¹⁸O content in compound **7**.

A natural bond orbital (NBO) analysis (Table 2) shows that the P=O→M electron density transfer is higher for M = Si than for M = Sn and reveals occupation of the formal empty p-orbitals by 0.292 and 0.198 au, respectively. Thus, the intramolecular coordination decreases the electrophilicity of the tin atom in cation **3b** and even more of the silicon atom in cation **6**. Consequently, attack of water at silicon in cation **6** is even less likely than at tin in cation **3b** with the consequence that path 3 can be ruled out to be responsible for the ¹⁸O content in the benzoxaphosphasilole **7**. Noteworthy, the atomic charges at carbon and oxygen of the OEt groups are almost identical in all compounds, but the positive atomic charge at phosphorus and hence its electrophilicity increase in the sequence 1-*t*-Bu-3,5-[P(O)(OEt)₂]₂-C₆H₃ < {4-*t*-Bu-2,6-[P(O)(OEt)₂]₂C₆H₂}SnPh₂⁺ < {4-*t*-Bu-2,6-[P(O)(OEt)₂]₂C₆H₂}SiPh₂⁺ with the difference between the tin and silicon derivatives being rather small (Table 2).

One possible explanation to account for the experimental results is the following.

The nucleophilic attack at the tetracoordinated phosphorus atom is known to require pseudorotation in order

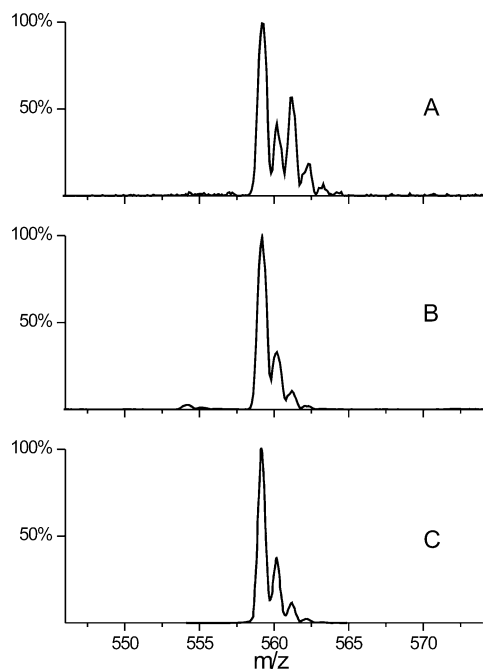


Figure 2. Electrospray mass spectra (ESMS) of 7-H resulting from reaction of (A) **6** + H₂¹⁸O (95%), (B) **6** + H₂O (natural isotope distribution), and (C) **6** + H₂O (calculated for natural isotope distribution).

to follow the axial-entrance–axial-departure principle.^{22–29} For compounds containing phosphorus atoms as part of a five-membered ring such pseudorotation involves energetically less favored intermediates/transition states. Our results indicate that for the intramolecularly coordinated triorganosilicon cation **6** the attack of water at phosphorus and at the POC-carbon, respectively, must proceed at comparable rates, which in turn means that the axial-entrance–axial-departure principle does not hold here or that the activation barrier for pseudorotation at phosphorus is lower for compounds containing phosphorus and silicon in a five-membered ring (**M2**, M = Si, Scheme 2) than for related compounds containing phosphorus and tin (**M2**, M = Sn, Scheme 2). In the latter case, as stated above, only the attack of water at the POC-carbon results in formation of the benzoxaphosphastannoles **4a** and **4b**. A third possibility involves opening of the ring and unrestricted pseudorotation. However, this is rather unlikely, as the more ionic Sn–O bond is expected to open more easily than the Si–O bond.

Conclusion

The intramolecularly coordinated triorganotin hexafluorophosphates **3a** and **3b** and the related triorganosilicon derivative **6** can be seen as model compounds for

intermediates along the Lewis acid-catalyzed hydrolysis of aryl phosphonic esters. Although the experimental as well as the theoretical data at hand do not provide a straightforward picture of the mechanisms giving the benzoxaphosphastannole derivatives **4a** and **4b** and the benzoxaphosphasilole derivative **7**, respectively, it is evident that these mechanisms are influenced by the identity of the element M in {4-*t*-Bu-2,6-[P(O)(OEt)₂]₂-C₆H₂}MPh₂⁺ (M = Si, Sn).

Experimental Section

General Procedures. All solvents were dried and purified by standard procedures. All reactions were carried out under argon atmosphere using Schlenk techniques.

IR spectra (cm⁻¹) were recorded on a Bruker IFS 28 spectrometer. Bruker DPX-300 and DRX-400 spectrometers were used to obtain ¹H (400.13 MHz), ¹³C (100.63 MHz), ¹⁹F (282.36 MHz), ³¹P (121.49 MHz, 161.98 MHz), and ¹¹⁹Sn (111.92 MHz, 149.18 MHz) NMR spectra. ¹H, ¹³C, ¹⁹F, ³¹P, and ¹¹⁹Sn NMR chemical shifts δ are given in ppm and were referenced to Me₄Si (¹H, ¹³C), CCl₃F (¹⁹F), Me₄Sn (¹¹⁹Sn), and H₃PO₄ (85%, ³¹P), respectively. NMR spectra were recorded at room temperature unless otherwise stated. The assignment of the ¹³C resonances was achieved by ¹³C–³¹P 2D NMR with a triple resonance probehead. ³¹P was the detected nucleus, and the HMQC pulse program was used.³⁰ MAS NMR spectra were obtained on a Bruker MSL 400 spectrometer using cross-polarization and high-power proton decoupling (conditions: recycle delay 4.0–6.0 s, 90° pulse 5.0 μs, contact time 3.5 ms). Spinning rates of 4.5–7.0 kHz were employed. Each sample was measured with two independent spinning rates in order to identify the isotropic chemical shift. For ¹¹⁹Sn MAS NMR spectra *cyclo*-Hex₄Sn served as a second reference (–97.35 ppm against Me₄Sn).

Elemental analyses were performed on a LECO-CHNS-932 analyzer. Electrospray mass spectra were recorded in the positive mode on a Thermoquest-Finnigan instrument using CH₃CN as the mobile phase. The samples were introduced as solution in CH₃CN (*c* = 10⁻⁴ mol L⁻¹) via a syringe pump operating at 5–10 μL min⁻¹. The capillary voltage was varied between 1.4 and 10.0 V, while the coneskimmer voltage was varied between 106.6 and 159.3 V. Identification of the inspected ions was assisted by comparison of experimental and calculated isotope distribution patterns. The *m/z* values reported correspond to those of the most intense peaks in the corresponding isotope pattern.

{[4-*tert*-Butyl-2,6-bis(diethoxyphosphinyl)]phenyl}diphenylsilicon hexafluorophosphate (**5**) was prepared as previously reported.³ The synthesis and molecular structure of the arylbisphosphonic ester 1-*t*-Bu-3,5-[P(O)(*O*-Pr)₂]₂C₆H₃ will be described in a forthcoming paper.³¹ The atom-numbering scheme for **2a**, **3a**, **4a**, and **7** is given in Chart 3.

Molecular Orbital Calculations. Calculations of the structures and energies of 1-*t*-Bu-3,5-[P(O)(OEt)₂]₂C₆H₃ and {4-*t*-Bu-2,6-[P(O)(OEt)₂]₂C₆H₂}MPh₂⁺ (M = Sn, Si) have been carried out at the density functional (B3LYP) level with the Gaussian 98 program³² using the internal stored LANL2DZ basis set. This basis set was previously shown to be appropriate for large organotin compounds including intra- and intermolecular coordination,^{33–37} but nevertheless the geometry optimization of the P=O bond lengths is inaccurate. Comparing the results obtained by single-crystal X-ray structure analyses with those obtained by calculations, a systematic error of about 6% is observed for both {4-*t*-Bu-2,6-[P(O)(OEt)₂]₂C₆H₂}SnPh₂⁺ and 1-*t*-Bu-3,5-[P(O)(OEt)₂]₂C₆H₃.¹⁸ Note-

(22) Kyba, E. P. *J. Am. Chem. Soc.* **1975**, *97*, 2554.

(23) Kyba, E. P. *J. Am. Chem. Soc.* **1976**, *98*, 4805.

(24) Corriu, R. J. P.; Dutheil, J. P.; Lanneau, G. F.; Ould-Kada, S. *Tetrahedron* **1979**, *35*, 2889.

(25) Corriu, R. J. P.; Lanneau, G. F.; Leclercq, D. *Tetrahedron* **1980**, *36*, 1617.

(26) Corriu, R. J. P.; Dutheil, J. P.; Lanneau, G. F. *Tetrahedron* **1981**, *37*, 3681.

(27) Corriu, R. J. P.; Dutheil, J. P.; Lanneau, G. F. *J. Am. Chem. Soc.* **1984**, *106*, 1060.

(28) Corriu, R. J. P.; Lanneau, G. F.; Leclercq, D. *Tetrahedron* **1986**, *42*, 5591.

(29) Westheimer, F. H. *Acc. Chem. Res.* **1968**, *1*, 70.

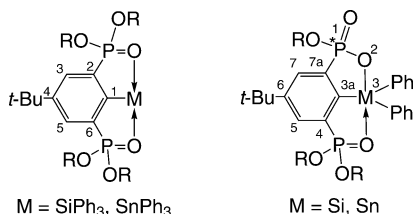
(30) Braun, S.; Kalinowski, H.-O.; Berger, S. *150 and More Basic NMR Experiments*; Wiley-VCH: New York, 1998.

(31) Henn, M.; Jurkschat, K.; Mahieu, B.; Mehring, M.; Müller, D.; Schürmann, M. Manuscript to be published.

Table 2. Selected Results of the NBO Analysis for 1-*t*-Bu-3,5-[P(O)(OEt)₂]₂C₆H₃ (RH), {4-*t*-Bu-2,6-[P(O)(OEt)₂]₂C₆H₂}SnPh₂⁺ (RSnPh₂⁺), and {4-*t*-Bu-2,6-[P(O)(OEt)₂]₂C₆H₂}SiPh₂⁺ (RSiPh₂⁺) Calculated at the B3LYP/LANL2DZ Level of Theory (atomic charges; charge transfer, au; orbital occupation, au)

	NBO charges				charge transfer P=O→M	occ(p(M))
	P	P=O	M	O-C		
RH	+2.282	-1.053		+0.039	-0.964 to -0.979	
RSnPh ₂ ⁺	+2.355	-1.158	+2.350	+0.049 to +0.054	-0.965 to -0.982	0.122
RSiPh ₂ ⁺	+2.361	-1.159				
	+2.365	-1.122	+2.014	+0.052 to +0.057	-0.965 to -0.985	0.183
	+2.372	-1.126				0.292

Chart 3



worthy, using the same method with a basis set such as 6-311+G* the description of P=O bond lengths in arylphosphonic esters does not become significantly better. Having these results in mind and being forced to use the same level of theory for all compounds to get comparable results, the LANL2DZ basis set was chosen. Additionally, the wave functions were analyzed by the natural bond orbital (NBO) method,^{38–40} a standard option of Gaussian 98. The NBO analysis explains the strength of coordinative bonds in terms of donor–acceptor interactions between doubly occupied lone pair orbitals and unoccupied antibonding orbitals and provides atomic charges that are more reliable than Mulliken charges.

Crystallography. A single crystal suitable for X-ray analysis was directly taken from the reaction mixture and sealed with some dry paraffin oil. Crystal data and structure solution of **3a**: [C₃₄H₄₉O₆P₂Sn]⁺[PF₆]⁻, *M*_r = 879.33, triclinic in *P* $\bar{1}$, *a* = 11.557(1) Å, *b* = 13.836(1) Å, *c* = 14.534(1) Å, α = 107.962(1)°, β = 106.836(1)°, γ = 100.699(1)°, *V* = 2017.2(3) Å³, *Z* = 2, *D*_x = 1.448 Mg/m³, *F*(000) = 900, λ (Mo K α) = 0.71069 Å, μ = 0.820 mm⁻¹, *T* = 200(1) K. The data were collected to a maximum θ = 25.03° with 360 frames via ω -rotation ($\Delta\omega$ = 1°) at two times 10 s per frame on a Nonius Kappa CCD diffractometer with a completeness of 86.9% to θ_{\max} . The structure was solved by direct methods using SHELXS97⁴¹ and successive difference Fourier syntheses and was refined by full-

matrix least-squares calculations using all measured *F*² data and SHELXL97.⁴² All non-H atoms were refined anisotropically. The H atoms were placed in geometrically calculated positions using a riding model and refined with common isotropic temperature factors for different C–H types (C–H_{prim}, 0.96 Å, C–H_{tert}, 0.98 Å, *U*_{iso} 0.066(2) Å²; H_{aryl} C–H 0.93 Å, *U*_{iso} 0.046(3) Å²). All *F* atoms of the [PF₆]⁻ are disordered over two positions with occupancies of 0.5. Atomic scattering factors for neutral atoms and real and imaginary dispersion terms were taken from International Tables for X-ray Crystallography.⁴³ *R*₁ = 0.0348 for 4514 [*I* > 2 σ (*I*)] and *wR*₂ = 0.0765 for 6202 independent reflections. The max. and min. residual electron densities were 0.398 and -0.898 e⁻Å⁻³.

[[4-*tert*-Butyl-2,6-bis(di-isopropoxyphosphiny)]phenyl]-triphenylstannane (2a). To a solution of 1-*tert*-butyl-3,5-bis(di-isopropoxyphosphiny)benzene (3.00 g, 6.5 mmol) in diethyl ether/*n*-hexane (50 mL, 2:1) was added dropwise, at -40 °C, LiN*i*-Pr₂ in cyclohexane (6 mL, 1.5 M). The reaction mixture was stirred for 4 h at this temperature. To the solution was added portionwise, at -25 °C, triphenyltin chloride (4.10 g, 10.6 mmol). The reaction mixture was stirred for another 14 h (-25 °C to room temperature), the precipitate was filtered, and the solvent was evaporated in vacuo. Crystallization from *n*-hexane (500 mL) afforded 2.90 g (55%) of **2a** as colorless crystals, mp 174–178 °C. ¹H NMR (C₆D₆): δ 0.74 [d, ³*J*(¹H–¹H) = 6.2 Hz, 12H; C(CH₃)(CH₃)'], 1.10 [d, ³*J*(¹H–¹H) = 6.2 Hz, 12H; C(CH₃)(CH₃)'], 1.38 (s, 9H; CH₃), 3.96–4.07 (complex pattern, 4H; OCH), 7.12–7.24 (complex pattern, 9H; H_{Ph}), 7.55–7.69 (complex pattern, 6H; H_{Ph}), 7.91–7.97 (complex pattern, 2H; H_{arom}). ¹³C{¹H} NMR (CDCl₃): δ 23.2 (complex pattern, 4C; C(CH₃)(CH₃')), 23.7 (complex pattern, 4C; C(CH₃)(CH₃')), 30.8 (s, 3C; C(CH₃)), 34.6 (s, 1C; C(CH₃)), 70.5 (complex pattern, 4C; OCH), 126.9 [s, ⁴*J*(¹³C–¹¹⁹Sn) = 11 Hz, 3C; C_p], 127.4 [s, ³*J*(¹³C–¹¹⁹Sn) = 54 Hz, 6C; C_m], 133.3 (complex pattern, 2C; C_{3,5}), 136.8 [s, ²*J*(¹³C–¹¹⁹Sn) = 38 Hz, 6C; C_o], 139.2 [dd, ¹*J*(¹³C–³¹P) = 211 Hz, ³*J*(¹³C–³¹P) = 20 Hz, 2C; C_{2,6}], 146.9 [s, ¹*J*(¹³C–¹¹⁹Sn) = 596/570 Hz, 3C; C_i], 150.6 [t, ²*J*(¹³C–³¹P) = 13 Hz, 1C; C₁], 151.4 [t, ³*J*(¹³C–³¹P) = 22 Hz, 1C; C₄]. ³¹P{¹H} NMR (161.98 MHz, CDCl₃): δ 17.4 [s, ²*J*(³¹P–¹¹⁹Sn) = 35 Hz], ¹¹⁹Sn{¹H} NMR (149.18 MHz): δ -184.0 [t, ¹*J*(¹¹⁹Sn–³¹P) = 34 Hz]. IR (KBr): $\tilde{\nu}$ (P=O) 1242 cm⁻¹. Anal. Calcd for C₄₀H₅₄O₆P₂Sn: C, 59.2; H, 6.7. Found: C, 59.4; H, 6.5.

[[4-*tert*-Butyl-2,6-bis(di-isopropoxyphosphiny)]phenyl]-diphenylstannyl Hexafluorophosphate (3a). To a solution of [[4-*tert*-butyl-2,6-bis(di-isopropoxyphosphiny)]phenyl]triphenylstannane (**2a**) (0.36 g, 0.44 mmol) in toluene (5 mL) was added triphenylcarbonium hexafluorophosphate (0.17 g, 0.44 mmol). The reaction mixture was stirred at 60 °C for 48 h. Cooling to 0 °C yielded 0.23 g (54%) of **3a** as colorless crystals, decomposition at 167 °C. ¹H NMR (C₆D₆): δ 1.20 [d, ³*J*(¹H–¹H) = 6.3 Hz, 12H; C(CH₃)(CH₃)'], 1.31 [d, ³*J*(¹H–¹H) = 6.3 Hz, 12H; C(CH₃)(CH₃)'], 1.38 (s, 9H; CH₃), 4.56–4.67 (complex pattern, 4H; OCH), 7.41–7.44 (complex pattern, 6H; H_{Ph}), 7.55–7.74 (complex pattern, 4H; H_{Ph}), 8.03–8.10 (complex

(32) Frisch, M. J.; Trucks, G. W.; Schlegel, H. B.; Scuseria, G. E.; Robb, M. A.; Cheeseman, J. R.; Zakrzewski, V. G.; Montgomery, J. A.; Stratmann, R. E.; Burant, J. C.; Dapprich, S.; Millian, J. M.; Daniels, A. D.; Kudin, K. N.; Strain, M. C.; Farkas, O.; Tomasi, J.; Barone, V.; Cossi, M.; Cammi, R.; Mennucci, B.; Pomelli, C.; Adamo, C.; Clifford, S.; Ochterski, J.; Petersson, G. A.; Ayala, P. Y.; Cui, Q.; Morokuma, K.; Malick, D. K.; Rabuck, A. D.; Raghavachari, K.; Foresman, J. B.; Cioslowski, J.; Ortiz, J. V.; Stefanov, B. B.; Liu, G.; Liashenko, A.; Piskorz, P.; Komaromi, I.; Bomperts, R.; Martin, R. L.; Fox, D. J.; Keith, T.; Al-Laham, M. A.; Peng, C. Y.; Nanayakkara, A.; Gonzalez, C.; Challacombe, M.; Gill, P. M. W.; Johnson, B. G.; Chen, W.; Wong, M. W.; Andres, J. L.; Head-Gordon, M.; Replogle, E. S.; Pople, J. A. *Gaussian 98*; Gaussian Inc.: Pittsburgh, 1998.

(33) Buntine, M. A.; Hall, V. J.; Kosovel, F. J.; Tiekink, E. R. T. *J. Phys. Chem. A* **1998**, *102*, 2472.

(34) Obora, Y.; Nakanishi, M.; Tokunaga, M.; Tsuji, Y. *J. Org. Chem.* **2002**, *67*, 5835.

(35) Ryner, M.; Finne, A.; Albertsson, A.-C.; Kricheldorf, H. R. *Macromolecules* **2001**, *34*, 7281.

(36) Hu, Y.-H.; Su, M.-D. *J. Phys. Chem. A* **2003**, *107*, 4130.

(37) Tani, K.; Kato, S.; Kanda, T.; Inagaki, S. *Org. Lett.* **2001**, *3*, 655.

(38) Reed, A. E.; Curtiss, L. A.; Weinhold, F. *Chem. Rev.* **1988**, *88*, 899.

(39) King, B. F.; Weinhold, F. *J. Chem. Phys.* **1995**, *103*, 333.

(40) *NBO 4.0 Program Manual*; University of Wisconsin Theoretical Chemistry Institute Technical Report WISC-TCI-756.

(41) Sheldrick, G. M. *Acta Crystallogr. A* **1990**, *46*, 467.

(42) Sheldrick, G. M. *SHELXL97*; University of Göttingen: Germany, 1997.

(43) *International Tables for Crystallography*; Kluwer Academic Publishers: Dordrecht, The Netherlands, 1992; Vol. C.

pattern, 2H; H_{arom}). $^{13}\text{C}\{^1\text{H}\}$ NMR (CDCl_3): δ 23.4–23.6 (unresolved, 8C; $\text{C}(\text{CH}_3)(\text{CH}_3')$), 30.9 (s, 3C; $\text{C}(\text{CH}_3)_3$), 35.6 (s, 1C; $\text{C}(\text{CH}_3)_3$), 76.2 (complex pattern, 4C; OCH), 129.3 [s, $^3J(^{13}\text{C}-^{119}\text{Sn}) = 78$ Hz, 4C; C_m], 131.2 [s, $^4J(^{13}\text{C}-^{119}\text{Sn}) = 16$ Hz, 2C; C_p], 132.0 [dd, $^1J(^{13}\text{C}-^{31}\text{P}) = 173$ Hz, $^3J(^{13}\text{C}-^{31}\text{P}) = 18$ Hz, 2C; $\text{C}_{2,6}$], 132.6 (complex pattern, 2C; $\text{C}_{3,5}$), 135.3 [s, $^2J(^{13}\text{C}-^{119}\text{Sn}) = 53$ Hz, 4C; C_o], 146.7 (s, 2C; C_j), 154.1 [t, $^2J(^{13}\text{C}-^{31}\text{P}) = 20$ Hz, 1C; C_4], 157.2 [t, $^3J(^{13}\text{C}-^{31}\text{P}) = 13$ Hz, 1C; C_1]. $^{31}\text{P}\{^1\text{H}\}$ NMR (161.98 MHz, CDCl_3): δ 26.1 [s, $J(^{31}\text{P}-^{119}\text{Sn}) = 4$ Hz], -143.7 (septet, PF_6^-). $^{31}\text{P}\{^1\text{H}\}$ MAS NMR (161.98 MHz): δ 21.9, -143.6. $^{119}\text{Sn}\{^1\text{H}\}$ NMR (149.18 MHz): δ -207.8 [t, $J(^{119}\text{Sn}-^{31}\text{P}) = 5$ Hz]. $^{119}\text{Sn}\{^1\text{H}\}$ MAS NMR (149.21 MHz): δ -200.4. IR (KBr): $\tilde{\nu}(\text{P}=\text{O})$ 1177 cm^{-1} . Anal. Calcd for $\text{C}_{34}\text{H}_{49}\text{F}_6\text{O}_6\text{P}_3\text{Sn}$: C, 46.4; H, 5.6. Found: C, 46.8; H, 5.7.

In Situ Preparation of [4-*tert*-Butyl-2,6-bis(diethoxyphosphinyl)phenyl]diphenylstannyl Hexafluorophosphate (3b). To a solution of [4-*tert*-butyl-2,6-bis(diethoxyphosphinyl)phenyl]triphenylstannane (**2b**) (0.12 g, 0.16 mmol) in toluene (15 mL) was added triphenylcarbonium hexafluorophosphate (0.062 g, 0.16 mmol). The reaction mixture was stirred at 65 °C for 24 h. The completeness of the reaction was controlled by NMR spectroscopy. $^{31}\text{P}\{^1\text{H}\}$ NMR (121.49 MHz, CDCl_3): δ 30.1 [s, $J(^{31}\text{P}-^{119}\text{Sn}) = 4$ Hz, integral 72%], -18.9 (t, integral 6%), -143.7 (septet, PF_6^- , integral 20%). $^{119}\text{Sn}\{^1\text{H}\}$ NMR (111.92 MHz): δ -203.3.

6-*tert*-Butyl-4-di-isopropoxyphosphinyl-1-ethoxy-1-oxo-3,3-diphenyl-2,1,3-benzoxaphosphastannole (4a). Method A: To a solution of [4-*tert*-butyl-2,6-bis(di-isopropoxyphosphinyl)phenyl]triphenylstannane (**2a**) (200 mg, 0.25 mmol) in dichloromethane (30 mL) was added dropwise, at 0 °C, Br_2 in dichloromethane (0.87 mL, 0.39 M). The solution was stirred for 48 h at room temperature. After evaporation of the solvent the residue was dissolved in toluene (30 mL) and heated at reflux for 2 h. Evaporation of the solvent and crystallization of the residue from dichloromethane/*n*-hexane (1:1) afforded 156 mg (90%) of **4a** as a colorless solid, mp 141–142 °C. Method B: To a solution of [4-*tert*-butyl-2,6-bis(di-isopropoxyphosphinyl)phenyl]triphenylstannane (**2a**) (200 mg, 0.25 mmol) in dichloromethane (10 mL) was added portionwise, at 0 °C, I_2 (90 mg, 0.35 mmol). The solution was stirred for 48 h at room temperature. After addition of saturated aqueous NaHCO_3 (2 mL) the solution was stirred for 24 h at room temperature and heated at reflux for 22 h. The organic layer was separated and dried over Na_2SO_4 . Filtration of Na_2SO_4 , evaporation of the solvent, and crystallization of the residue from diethyl ether/*n*-hexane (1:1) afforded 124 mg (72%) of **4a** as a colorless solid, mp 141–142 °C. ^1H NMR (CDCl_3): δ 0.90 [d, $^3J(\text{H}-^1\text{H}) = 6.2$ Hz, 3H; $\text{C}(\text{CH}_3)(\text{CH}_3')$ (P)], 1.12 [d, $^3J(\text{H}-^1\text{H}) = 6.4$ Hz, 3H; $\text{C}(\text{CH}_3)(\text{CH}_3')$ (P)], 1.18 [d, $^3J(\text{H}-^1\text{H}) = 6.2$ Hz, 3H; $\text{C}(\text{CH}_3)(\text{CH}_3')$ (P)], 1.23 [d, $^3J(\text{H}-^1\text{H}) = 6.0$ Hz, 3H; $\text{C}(\text{CH}_3)(\text{CH}_3')$ (P*)], 1.28 [d, $^3J(\text{H}-^1\text{H}) = 6.0$ Hz, 3H; $\text{C}(\text{CH}_3)(\text{CH}_3')$ (P)], 1.30 [d, $^3J(\text{H}-^1\text{H}) = 6.3$ Hz, 3H; $\text{C}(\text{CH}_3)(\text{CH}_3')$ (P*)], 1.31 (s, 9H; CH_3), 4.10–4.21 (complex pattern, 1H; OCH (P)), 4.41–4.52 (complex pattern, 1H; OCH (P)), 4.64–4.75 (complex pattern, 1H; OCH (P*)), 7.29–7.35 (complex pattern, 6H; $H_{m/p}$), 7.76 (complex pattern, 1H; H_{c-s}), 7.80–7.83 (complex pattern, 2H; H_o), 7.90–7.92 (complex pattern, 2H; H_o), 8.22 (complex pattern, 1H; H_{c-7}). $^{13}\text{C}\{^1\text{H}\}$ NMR (CDCl_3): δ 23.2 [d, $^3J(^{13}\text{C}-^{31}\text{P}) = 5$ Hz, 1C; $\text{C}(\text{CH}_3)(\text{CH}_3')$ (P)], 23.5 [d, $^3J(^{13}\text{C}-^{31}\text{P}) = 4$ Hz, 1C; $\text{C}(\text{CH}_3)(\text{CH}_3')$ (P)], 23.5 [d, $^3J(^{13}\text{C}-^{31}\text{P}) = 6$ Hz, 1C; $\text{C}(\text{CH}_3)(\text{CH}_3')$ (P)], 23.7 [d, $^3J(^{13}\text{C}-^{31}\text{P}) = 4$ Hz, 1C; $\text{C}(\text{CH}_3)(\text{CH}_3')$ (P)], 24.3 [d, $^3J(^{13}\text{C}-^{31}\text{P}) = 6$ Hz, 1C; $\text{C}(\text{CH}_3)(\text{CH}_3')$ (P*)], 24.3 [d, $^3J(^{13}\text{C}-^{31}\text{P}) = 4$ Hz, 1C; $\text{C}(\text{CH}_3)(\text{CH}_3')$ (P*)], 31.1 (s, 3C; $\text{C}(\text{CH}_3)_3$), 35.2 (s, 1C; $\text{C}(\text{CH}_3)_3$), 68.9 [d, $^2J(^{13}\text{C}-^{31}\text{P}) = 6$ Hz, 1C; OCH (P*)], 73.1 [d, $^2J(^{13}\text{C}-^{31}\text{P}) = 5$ Hz, 1C; OCH (P)], 73.4 [d, $^2J(^{13}\text{C}-^{31}\text{P}) = 5$ Hz, 1C; OCH (P)], 128.4 [s, $^3J(^{13}\text{C}-^{119}\text{Sn}) = 71$ Hz, 2C; C_m], 128.4 [s, $^3J(^{13}\text{C}-^{119}\text{Sn}) = 76$ Hz, 2C; C_m], 129.1 [dd, $^2J(^{13}\text{C}-^{31}\text{P}) = 12$ Hz, $^4J(^{13}\text{C}-^{31}\text{P}) = 3$ Hz, 1C; C_5], 129.8 [s, $^4J(^{13}\text{C}-^{31}\text{P}) = 16$ Hz, 2C; C_p], 130.3 [dd, $^1J(^{13}\text{C}-^{31}\text{P}) = 112$ Hz, $^3J(^{13}\text{C}-^{31}\text{P}) = 16$ Hz, 1C; C_4], 131.9 [dd, $^2J(^{13}\text{C}-^{31}\text{P}) = 12$ Hz, $^4J(^{13}\text{C}-^{31}\text{P}) = 4$ Hz,

1C; C_7], 135.8 [s, $^2J(^{13}\text{C}-^{119}\text{Sn}) = 52$ Hz, 2C; C_o], 136.1 [s, $^2J(^{13}\text{C}-^{119}\text{Sn}) = 50$ Hz, 2C; C_o], 138.3 [t, $J(^{13}\text{C}-^{31}\text{P}) = 3$ Hz, 1C; C_j], 139.1 [t, $J(^{13}\text{C}-^{31}\text{P}) = 3$ Hz, 1C; C_j], 141.4 [dd, $^1J(^{13}\text{C}-^{31}\text{P}) = 177$ Hz, $^3J(^{13}\text{C}-^{31}\text{P}) = 17$ Hz, 1C; C_{7a}], 153.0 [pseudo-t, $^2J(^{13}\text{C}-^{31}\text{P}) = 17$ Hz, 1C; C_6], 154.7 [dd, $J(^{13}\text{C}-^{31}\text{P}) = 11$ Hz, $J(^{13}\text{C}-^{31}\text{P}) = 13$ Hz, 1C; C_{3a}]. $^{31}\text{P}\{^1\text{H}\}$ NMR (161.98 MHz, CDCl_3): δ 17.7 [d, $^4J(^{31}\text{P}-^{31}\text{P}) = 4$ Hz, $J(^{31}\text{P}-^{119}\text{Sn}) = 23$ Hz; P*], 26.2 [d, $^4J(^{31}\text{P}-^{31}\text{P}) = 4$ Hz, $J(^{31}\text{P}-^{119}\text{Sn}) = 25$ Hz; P]. $^{31}\text{P}\{^1\text{H}\}$ MAS NMR (161.98 MHz): δ 13.7, 26.0. $^{119}\text{Sn}\{^1\text{H}\}$ NMR (149.18 MHz): δ -223.4 [dd, $J(^{119}\text{Sn}-^{31}\text{P}) = 18/23$ Hz]. $^{119}\text{Sn}\{^1\text{H}\}$ MAS NMR (149.21 MHz): δ -211.9. IR (KBr): $\tilde{\nu}(\text{P}=\text{O})$ 1171 cm^{-1} , 1154 cm^{-1} . Anal. Calcd for $\text{C}_{31}\text{H}_{42}\text{O}_6\text{P}_2\text{Sn}$: C, 53.9; H, 6.1. Found: C, 53.7; H, 6.4.

Reaction of [4-*tert*-Butyl-2,6-bis(di-isopropoxyphosphinyl)phenyl]diphenylstannyl Hexafluorophosphate (3a) with H_2^{18}O . To 9 mL of a solution of [4-*tert*-butyl-2,6-bis(di-isopropoxyphosphinyl)phenyl]diphenylstannane hexafluorophosphate (**3a**) in toluene (0.011 M) was added H_2^{18}O (20 μL). After the reaction mixture was stirred at 75–80 °C for 2 days, the completeness of the reaction was controlled by ^{31}P NMR spectroscopy. ESMS: $m/z = 693.1$ (**4a**-H corresponding to natural isotope distribution).

Reaction of [4-*tert*-Butyl-2,6-bis(diethoxyphosphinyl)phenyl]diphenylstannyl Hexafluorophosphate (3b) with H_2^{18}O . To 5 mL of a solution of [4-*tert*-butyl-2,6-bis(diethoxyphosphinyl)phenyl]diphenylstannane hexafluorophosphate (**3b**) in toluene (0.01 M) was added H_2^{18}O (50 μL). After the reaction mixture was stirred at 70 °C for 2 days, the completeness of the reaction was controlled by ^{31}P NMR spectroscopy. ESMS: $m/z = 651.1$ (**4b**-H corresponding to natural isotope distribution).

Reaction of [4-*tert*-Butyl-2,6-bis(di-isopropoxyphosphinyl)phenyl]diphenylstannyl Hexafluorophosphate (3a) with Ph_4PBr . To a solution of [4-*tert*-butyl-2,6-bis(di-isopropoxyphosphinyl)phenyl]diphenylstannyl hexafluorophosphate (**3a**) (36.7 mg, 4.2×10^{-6} mol) in 0.5 mL of toluene- d_8 was added tetraphenylphosphonium bromide, Ph_4PBr (17.5 mg, 4.2×10^{-6} mol). After the reaction mixture was stirred at 80 °C for 20 h the solution was characterized by NMR spectroscopy. ^{31}P NMR (161.98 MHz, $\text{tol}-d_8$): δ -10.6 (s, 1%), -4.8 (s, 1%), 16.5 [d, $^4J(^{31}\text{P}-^{31}\text{P}) = 3$ Hz; **4a**, 45%], 19.6 (A-H, 8%) 26.6 [d, $^4J(^{31}\text{P}-^{31}\text{P}) = 3$ Hz; **4a**, 45%].

Reaction of [4-*tert*-Butyl-2,6-bis(di-isopropoxyphosphinyl)phenyl]diphenylstannyl Hexafluorophosphate (3a) with Bu_4NF . To a solution of [4-*tert*-butyl-2,6-bis(di-isopropoxyphosphinyl)phenyl]diphenylstannyl hexafluorophosphate (**3a**) (0.14 g, 0.16 mmol) in 0.3 mL of CD_2Cl_2 were added well-defined quantities of tetrabutylammonium fluoride, $\text{Bu}_4\text{NF} \cdot 3\text{H}_2\text{O}$. The resulting solutions were characterized by NMR spectroscopy. $^{119}\text{Sn}\{^1\text{H}\}$ NMR (149.21 MHz, CD_2Cl_2 , 20 °C, pure **3a**): δ -207.7 [t, $J(^{119}\text{Sn}-^{31}\text{P}) = 5$ Hz]. $^{119}\text{Sn}\{^1\text{H}\}$ NMR (149.21 MHz, CD_2Cl_2 , 20 °C, **3a** + 0.10 mmol $\text{Bu}_4\text{NF} \cdot 3\text{H}_2\text{O}$): δ -209 ($\nu_{1/2} = 670$ Hz). $^{119}\text{Sn}\{^1\text{H}\}$ NMR (149.21 MHz, CD_2Cl_2 , -30 °C, **3a** + 0.10 mmol $\text{Bu}_4\text{NF} \cdot 3\text{H}_2\text{O}$): δ -211.4 ($\nu_{1/2} = 27$ Hz, 73%), 267.3 [dt, $J(^{119}\text{Sn}-^{31}\text{P}) = 37$ Hz, $^1J(^{119}\text{Sn}-^{19}\text{F}) = 2350$ Hz, 27%]. $^{119}\text{Sn}\{^1\text{H}\}$ NMR (149.21 MHz, CD_2Cl_2 , -30 °C, **3a** + 0.20 mmol $\text{Bu}_4\text{NF} \cdot 3\text{H}_2\text{O}$): δ -211.3 ($\nu_{1/2} = 24$ Hz, 42%), 267.7 [dt, $J(^{119}\text{Sn}-^{31}\text{P}) = 37$ Hz, $^1J(^{119}\text{Sn}-^{19}\text{F}) = 2353$ Hz, 58%]. $^{119}\text{Sn}\{^1\text{H}\}$ NMR (149.21 MHz, CD_2Cl_2 , 20 °C, **3a** + 0.40 mmol $\text{Bu}_4\text{NF} \cdot 3\text{H}_2\text{O}$): δ -266 ($\nu_{1/2} = 3000$ Hz). $^{119}\text{Sn}\{^1\text{H}\}$ NMR (149.21 MHz, CD_2Cl_2 , -30 °C, **3a** + 0.40 mmol $\text{Bu}_4\text{NF} \cdot 3\text{H}_2\text{O}$): δ 268.6 [dt, $J(^{119}\text{Sn}-^{31}\text{P}) = 40$ Hz, $^1J(^{119}\text{Sn}-^{19}\text{F}) = 2350$ Hz].

Reaction of [4-*tert*-Butyl-2,6-bis(di-isopropoxyphosphinyl)phenyl]diphenylstannyl Hexafluorophosphate (3a) with CsF . To a solution of [4-*tert*-butyl-2,6-bis(di-isopropoxyphosphinyl)phenyl]diphenylstannyl hexafluorophosphate (**3a**) (0.04 g, 0.05 mmol) in dry toluene (0.4 mL) was added an excess of cesium fluoride (0.01 g, 0.07 mmol). The suspension was sealed in an NMR tube and was heated at 80 °C for 48 h. The resulting suspension was characterized

by NMR spectroscopy. ^{31}P NMR (161.98 MHz, *tol-d*₆): δ -12.3 (s, 1%), -6.3 (s, 1%), 16.0 [d, $^4J(^{31}\text{P}-^{31}\text{P}) = 4$ Hz, $J(^{31}\text{P}-^{119}\text{Sn}) = 18$ Hz; **4a**, 47%], 16.5 (R-H, 4%) 26.5 [d, $^4J(^{31}\text{P}-^{31}\text{P}) = 4$ Hz, $J(^{31}\text{P}-^{119}\text{Sn}) = 25$ Hz; **4a**, 47%]. ^{19}F NMR (*tol-d*₆): δ -167.7 (doublet of heptet, $^2J(^{19}\text{F}-^1\text{H}) = 48$ Hz, $^3J(^{19}\text{F}-^1\text{H}) = 23$ Hz, *i*-PrF).

Reaction of [(4-*tert*-Butyl-2,6-bis(diethoxyphosphinyl))-phenyl]diphenylsiliconium Hexafluorophosphate (6**) with H_2^{18}O .** To a solution of in situ-prepared [(4-*tert*-butyl-2,6-bis(diethoxyphosphinyl))-phenyl]diphenylsiliconium hexafluorophosphate (**6**) in toluene (7 mL, 8.43 M) was added H_2^{18}O (50 μL). After the reaction mixture had been stirred at 60 °C for 5 days, the completeness of the reaction was controlled by ^{31}P NMR spectroscopy. ESMS: $m/z = 559.2$ (7-H, 559.2: 100%, 561.2: 55%).

Reaction of [(4-*tert*-Butyl-2,6-bis(diethoxyphosphinyl))-phenyl]diphenylsiliconium Hexafluorophosphate (6**) with**

H_2^{16}O . Experimental data compare H_2^{18}O -experiment. ESMS: $m/z = 559.2$ (7-H corresponding to natural isotope distribution, 559.2: 100%, 561.2: 11%).

Acknowledgment. We thank the Deutsche Forschungsgemeinschaft and the Fonds der Chemischen Industrie for financial support. Mrs U. Bünzli-Trepp (ETH Zurich, Switzerland) is gratefully acknowledged for help concerning the nomenclature of compounds reported in this paper.

Supporting Information Available: Crystal data for **3a**. This material is available free of charge via the Internet at <http://pubs.acs.org>.

OM0305061